

SPECIAL
ISSUE

LASSBio-1829 Hydrochloride: Development of a New Orally Active *N*-Acylhydrazone IKK2 Inhibitor with Anti-inflammatory Properties

Isabella A. Guedes,^[b] Rosana H. C. N. Freitas,^[a] Natália M. Cordeiro,^[c] Thaís S. do Nascimento,^[c] Tayna S. Valerio,^[c] Patrícia D. Fernandes,^[c] Laurent E. Dardenne,^[b] and Carlos A. M. Fraga*^[a]

Inhibitor of nuclear factor κ B kinase 2 (IKK2) is suggested to be a potential target for the development of novel anti-inflammatory and anticancer drugs. In this work, we applied structure-based drug design to improve the potency of the inhibitor (*E*)-*N'*-(4-nitrobenzylidene)-2-naphthohydrazide (LASSBio-1524, **1a**: IC₅₀ = 20 μ M). The molecular model built for IKK2 together with the docking methodology employed were able to provide important and consistent information with respect to the structural and chemical inhibitor characteristics that may confer po-

tency to IKK2 inhibitors, providing important guidelines for the development of a new *N*-acylhydrazone (NAH) derivative. (*E*)-*N'*-(4-(1*H*-pyrrolo[2,3-*b*]pyridin-4-yl)benzylidene)-2-naphthohydrazide hydrochloride (LASSBio-1829 hydrochloride, **10**) is a 7-azaindole NAH able to inhibit IKK2 with an IC₅₀ value of 3.8 μ M. LASSBio-1829 hydrochloride was found to be active in several pharmacological inflammation tests *in vivo*, showing its potential as an anti-inflammatory prototype.

Introduction

The IKK complex is formed by two catalytic subunits (the serine/threonine kinases, IKK1 and IKK2) and one regulatory subunit, IKK γ (or NEMO).^[1–3] This complex is involved in the activation of NF- κ B in response to apoptotic and inflammatory processes.^[4–6] Inhibition of the IKK complex is considered to be a promising approach for the treatment of chronic inflammation and cancer.^[7–13]

The IKK2 subunit participates in the activation of nuclear factor κ B (NF- κ B), which is essential for the full activation of this transcription factor. When a cell receives pro-inflammatory stimuli such as lipopolysaccharide (LPS) and tumor necrosis factor- α (TNF- α), IKK2 is activated by phosphorylation. Then, IKK2 phosphorylates the inhibitor of κ B (I κ B), which is associat-

ed with the dimers of NF- κ B in the cytosol. I κ B is polyubiquitinated and degraded, releasing the NF- κ B dimers. These dimers migrate into the cell nucleus, where they can exert their function as transcription factors assisting in the biosynthesis of pro-inflammatory cytokines.^[14] Activation of the biochemical cascades of NF- κ B is associated with the regulation of the innate and adaptive immune responses, among other physiological responses;^[15,16] however, continuous stimulation of NF- κ B is directly related with some types of inflammatory and autoimmune diseases, and also with the genesis and survival of tumor cells.^[17,18] In this context, IKK2 has been suggested to be a potential target for the development of novel candidates for anti-inflammatory and cancer drugs.^[19] The development of selective IKK2 inhibitors is necessary because the inhibition of IKK1 may promote severe side effects, especially within the epidermis.^[14,19–21]

The IKK2 subunit consists of three domains: the kinase, the ubiquitin-like and the dimerization domains.^[3] Nevertheless, only the kinase domain (residues 15–300) was modeled because the main focus of this work is the development of inhibitors that interact with the ATP binding site, which is located in this catalytic domain.

Currently, some IKK2 structures deposited in the Protein Data Bank (PDB codes 3RZF,^[22] 3QA8,^[22] 4E3C^[23] and 4KIK^[24]) have been solved at resolutions ranging from 2.8 to 4.0 Å. Despite their crucial role in elucidating some important structural and functional properties of IKK2, these structures do not have sufficient quality in the ATP binding site to be applied in the structure-based drug design of IKK2 inhibitors. The structure with the best resolution (PDB code 4KIK,^[24] solved at 2.83 Å)

[a] R. H. C. N. Freitas,⁺ Prof. C. A. M. Fraga
Laboratório de Avaliação e Substâncias Bioativas (LASSBio)
Instituto de Ciências Biomédicas (ICB)
Universidade Federal do Rio de Janeiro (UFRJ)
21941-902, Rio de Janeiro, RJ (Brazil)
E-mail: cmfraga@ccsdecania.ufrj.br

[b] I. A. Guedes,⁺ Prof. L. E. Dardenne
Laboratório Nacional de Computação Científica (LNCC/MCTI)
Petrópolis, RJ (Brazil)

[c] N. M. Cordeiro,⁺ T. S. d. Nascimento, T. S. Valerio, Prof. P. D. Fernandes
Laboratório de Farmacologia da Dor e da Inflamação
ICB, UFRJ, Rio de Janeiro, RJ (Brazil)

[*] These authors contributed equally to this work.

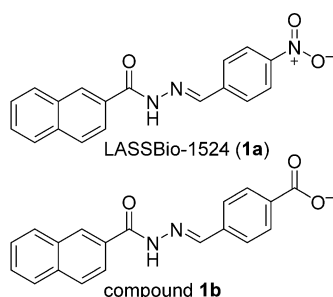
Supporting information for this article is available on the WWW under <http://dx.doi.org/10.1002/cmdc.201500266>.

SPECIAL
ISSUE

This article is part of a Special Issue on Drug Discovery in the Field of Autoimmune and Inflammatory Disorders. The complete issue can be browsed via Wiley Online Library.

has some disordered regions in the ATP binding site (e.g., G-loop), which might influence the docking results because this region is directly in contact with ATP and some inhibitors. For these reasons, the molecular model of the IKK2 isoform was constructed through a comparative modeling methodology based on multiple templates. The constructed model was validated through diverse energetic and geometric tools and also with the docking of ATP and other inhibitors from the literature.

Previous works from our research group reported the discovery of the *N*-acylhydrazone (NAH) derivative LASSBio-1524 (**1a**), a selective IKK2 inhibitor with $IC_{50}=20\ \mu\text{M}$ and active in pharmacological models of acute inflammation *in vivo*.^[25] In this study, the analogous compound **1b** is reported, which has a 4-carboxyphenyl ring, differing only at this point compared with LASSBio-1524, which has a 4-nitrophenyl ring. This modifi-



cation was deleterious, resulting in the inactivity of compound **1b**; however, the previous docking studies were not able to propose an explanation regarding this difference in activity.^[25]

In this work, we constructed a novel molecular model for the IKK2 kinase domain and carried out docking of compound **1b**, LASSBio-1524 (**1a**) and a set of diverse inhibitors from the literature to investigate the predicted binding properties that could justify their differential potency and selectivity. The aim of this work is to introduce structural modifications in the prototype of the NAH series, LASSBio-1524 (**1a**), guided by the docking results and *in vitro* experiments to obtain more potent and selective IKK2 inhibitors.

The structure-based drug design applied in our work led us to the development of LASSBio-1829 hydrochloride (**10**, $IC_{50}=3.8\ \mu\text{M}$), a more potent compound than the prototype of the NAH series LASSBio-1524 (**1a**, $IC_{50}=20\ \mu\text{M}$). LASSBio-1829 hydrochloride (**10**) was active against inflammation in several pharmacological tests *in vivo*, significantly reducing TNF- α and reactive oxygen species (ROS) biosynthesis, corroborating its potential as an anti-inflammatory prototype.

Results and Discussion

Structural modeling of IKK2

The geometric analyses performed with MolProbity indicated that the constructed model of IKK2 (Figure 1) presented no outlier residues, and the QMEAN and ProSA results showed satisfactory energetic and geometric quality (Supporting Information Figure S1).

As previously published and discussed,^[22,24] the IKK2 model shares a common folding pattern with other serine/threonine kinases: 1) a region rich in β -sheets (N terminus), and 2) a lobe rich in α -helices (C terminus), connected by 3) a hinge loop. The ATP binding site is located between the two lobes and is mainly formed by the hinge, G-loop, and A-loop regions (Figure 1).

The hinge is formed by two hydrogen bond acceptors (the oxygen atoms from the main chain of Glu97 and Cys99) and a hydrogen bond donor (the nitrogen atom from main chain of Cys99) (Figure 1A). The gatekeeper residue in IKK2 is a methionine (Met96), which is located between the end of the N-terminal lobe and the beginning of the hinge. Given the structural similarity between the members of the kinase family, this residue may undergo a conformational change in a similar fashion to the JNK3 enzyme, providing access to an allosteric binding site,^[26] however, further investigations are needed to confirm this hypothesis.

The G-loop, also known as the P-loop (phosphate binding loop), is a glycine-rich sequence followed by a conserved lysine and a serine/threonine and is located between the β_1 and the β_2 sheets. This loop acts as a lid of the ATP binding site, supporting phosphate transfer.^[27] In IKK2, the sequence of the G-loop consists of Gly24-Gly25-Phe26-Gly27.

The DFG sequence (Asp-Phe-Gly triad) is located in the A-loop and is highly conserved between the members of the kinase family; however, the IKK2 model has a DLG motif (formed by Asp-Leu-Gly residues) (Figure 1B). This finding is in

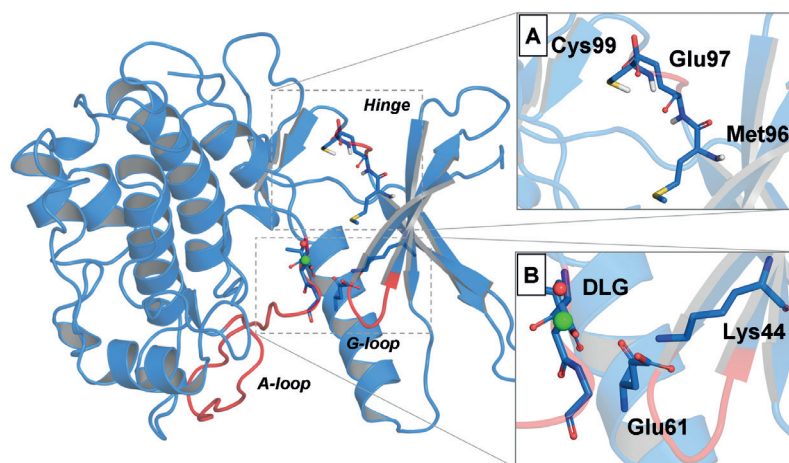


Figure 1. IKK2 molecular model. The regions of the hinge, A-loop, and G-loop are highlighted in red. A) Hinge region with the key amino acids Glu97 and Cys99, which form hydrogen bonds with the adenine ring of ATP and Met96. B) DLG triad residues (Asp166, Leu167, and Gly168), and the salt bridge between Lys44 and Glu61.

accordance with the amino acid sequence and with the 3D structures of IKK2, where the DLG motif is also present. The change of a phenylalanine to a leucine residue might consist of an important point of selectivity for the IKKs among other kinases.

The conserved pair of Lys44 (located in the β -sheet from the N-lobe) and Glu61 (located in the α -helix in the bottom of the binding site) forms a salt bridge in the IKK2 model, which is a feature of the active conformation of protein kinases (Figure 1B).^[28,29]

Validating the IKK2 model through the docking of ATP

The IKK2-ATP docking generated three top-ranked conformations with similar docking scores ranging from -16.511 to -16.040 kcal mol⁻¹. These conformations are very close with the experimental structure of the CDK2-ATP complex (PDB code 1HCK^[30], see Supporting Information Figure S2). The adenosine moiety interacts through two hydrogen bonds with the main chains of Glu97 and Cys99 of the hinge. These interactions are well conserved in the family of protein kinases.^[31] The ATP triphosphate group interacts with the Mg²⁺ and the main chain of the residues from the G-loop, whereas the ribose ring generally interacts with Asp103 through hydrogen bonds.

Molecular docking of inhibitors in IKK2

According to the docking results, a predominance of hydrogen bonds is observed between the inhibitors of IKK2 extracted from the literature and the hinge region, which is in accordance with the reported results for the ATP-competitive inhibitors of diverse protein kinases (Supporting Information Figure S3).^[32-34] In some cases, the inhibitors are able to interact through two or three hydrogen bonds with the hinge, most frequently with Glu97 and Cys99. The most potent inhibitors were observed to interact through two hydrogen bonds with the main chain of Cys99, including for the most potent inhibitor tested (compound **16**, IC₅₀ = 11 nM, see page S9 in Supporting Information). Potent inhibitors also usually interacted with other important and conserved residues in the ATP binding site, e.g., hydrogen bonds with Lys44 (from the β -sheet) and Asp166 (from the DLG motif).

The top-ranked poses of LASSBio-1524 (**1a**) and compound **1b** are shown in Figure 2. LASSBio-1524 (**1a**, Figure 2A) has

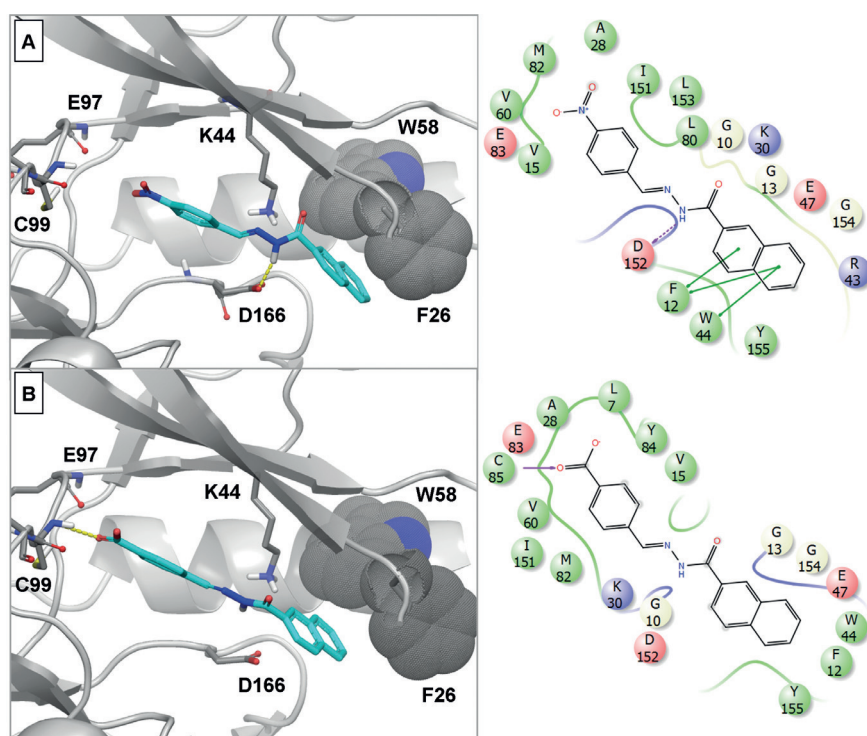


Figure 2. Predicted binding modes of A) LASSBio-1524 and B) compound **1b** found by docking experiments with IKK2 in the absence of water and metal ions. The aromatic side chains that interact with the inhibitor are represented as dots by the atomic van der Waals radii. The 2D ligand interaction diagrams generated with Maestro are shown at right; note: the residue position number labels on the 2D ligand interaction diagrams are shifted by $n-14$ relative to residue numbering at left and in the text.

a docking score of -4.27 kcal mol⁻¹ and exhibits the nitro group oriented toward the hinge region, the naphthyl group is located between the Mg²⁺ binding site and the G-loop, and the NAH group forms a hydrogen bond with Asp166. The naphthyl group interacts with Phe26 from the G-loop and Trp58 through stacking interactions. The predicted binding mode of compound **1b** (Figure 2B) has a docking score of -2.98 kcal mol⁻¹ and exhibits only a hydrogen bond between the carboxylate group and the hinge region (main chain NH of Cys99). Despite the overall similarity between the predicted binding modes of compound **1b** and LASSBio-1524, the former is not hydrogen bonded with Asp166 and loses the stacking interactions with Phe26 and Trp58.

The docking results guided us toward the development of the new NAH derivative by the positions of overlap between LASSBio-1524 (**1a**) and a potent and selective IKK2 inhibitor **2** (IC₅₀ = 66 nM, compound **3**^[35] in Table S2, Supporting Information), where it was observed that the ligands occupy and interact with different regions in the active site of the target enzyme (Figure 3). Thereby, LASSBio-1829 (**9**, Figure 4) was designed from a molecular hybridization between LASSBio-1524 (**1a**) and **2** as the optimization strategy. We kept the NAH subunit on account of it being a privileged structure,^[36] and thus it may contribute to the inhibitory activity. In subunit B, the bioisosteric exchange of the 2-aminopyrimidine ring by 7-azaindole (subunit B, Figure 4) was performed, once the azabicyclic system possessed the structural requirements needed to form

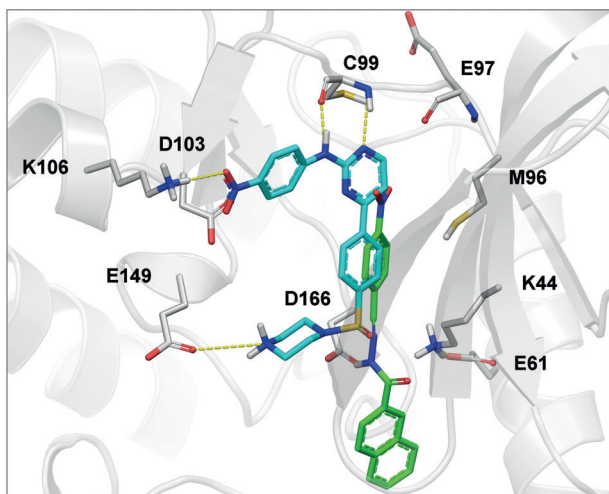


Figure 3. Overlap of the top-ranked docking pose of LASSBio-1524 (carbon atoms in green) and inhibitor **2**^[34] (carbon atoms in light blue) in the ATP binding site of IKK2. The hydrogen bonds formed by inhibitor **2** are shown as yellow dashes.

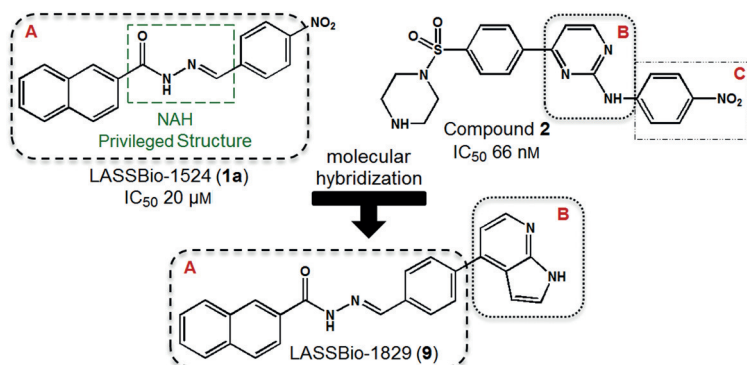


Figure 4. Design of LASSBio-1829 (**9**) from the molecular hybridization between LASSBio-1524 (**1a**) and compound **2**.^[35]

the same interactions that the 2-aminopyrimidine subunit possessed in the target enzyme, acting as hydrogen bond acceptor and donor. Additionally, subunit C (Figure 4) was removed for synthetic ease.

LASSBio-1829 (**9**, Figure 5) has one neutral and one protonated form predicted by Epik, with a predicted pK_a equal to 4.38 ± 1.47 (Figure 5B) and predicted state penalties of 0.0007 and 4.3996 kcal mol⁻¹ for the neutral and ionized forms, respectively. The neutral form of LASSBio-1829 has a better docking score than its ionized form (-9.719 and -1.595 kcal mol⁻¹). According to the docking results in the IKK2 model (Figure 5A), the neutral form of LASSBio-1829 shows the 7-azaindole group interacting through two hydrogen bonds with the Cys99 from the hinge, similar to the docking of compound **2**. Moreover, **9** maintains the hydrogen bonds with the key residues Lys44 and Asp166 as well as the stacking interactions with Phe26 from the G-loop, similar to the docking of LASSBio-1524 (**1a**, Figure 2A).

In addition to the observed structural quality of the constructed IKK2 model, the success of the docking experiment involving the ATP molecule (i.e., finding a very similar structure with the experimental one from the CDK2-ATP complex) is an important result to validate the docking protocol (structural quality of the model and the parameters of the docking program) used to predict the binding modes of the compounds investigated in this work.

The predicted binding modes of LASSBio-1524 (**1a**) and compound **1b** (Figure 2) share a similar orientation inside of the IKK2 binding site exhibiting the nitro and carboxylate groups oriented toward the hinge region. Unlike the most potent IKK2 inhibitors, LASSBio-1524 does not interact directly with the hinge region via a hydrogen bond (4.7 Å between the nitrogen atom of the nitro group and the oxygen of the main chain of Glu97, and 5.7 Å between the nitro group and the nitrogen atom of the main chain of Cys99), which may imply a low potency of this compound. This important result shows a way to modify this compound to improve its potency. On the other hand, the carboxyl group from compound **1b** is predicted to be closer and hydrogen bonded to the hinge; however, this negatively charged group is located in a hydrophobic region inside of the IKK2 binding site. Furthermore, the NAH group does not interact through hydrogen bonds with Lys44 or Asp166. These features might be reflected in the poor predicted score of this compound (-2.98 kcal mol⁻¹) and are probably associated with the fact that this compound is inactive against IKK2.

The most favorable docking score of the neutral LASSBio-1829 (**9**) (-9.72 kcal mol⁻¹), associated with the important interactions between 1) the 7-azaindole group and the hinge region, 2) the NAH group with the conserved Asp166 and Lys44, and 3) the stacking interactions with Phe26 from the G-loop (Figure 5), suggest that this compound may be more potent than the prototype of the series LASSBio-1524 (**1a**).

Chemistry

The synthesis of LASSBio-1829 (**9**) was carried out as outlined in Scheme 1. The starting material, 2-naphthoyl chloride **3**, was treated with methanol at room temperature to give the corresponding methyl ester **4**. Next, the ester **4** was reacted with hydrazine hydrate in ethanol under reflux to produce 2-naphthohydrazide **5**.^[37] The desired aldehyde **8** was obtained through a palladium-catalyzed cross-coupling reaction (Suzuki-Miyamura reaction).^[38] The Suzuki reaction is an efficient and economical method for synthesizing new C_{sp}²-C_{sp}² bonds, particularly in the synthesis of new leads.^[39,40] For this synthesis, appropriate aryl bromide **7** and formylbenzene boronic acid **6** reacted in the presence of sodium carbonate and palladium catalyst (PdCl₂(PPh₃)₂) in acetonitrile and water under microwave irradiation. After column chromatography, the aldehyde **8** was obtained in moderate yield.^[41] Next, the synthesized aldehyde **8** was condensed with 2-naphthohydrazide **5**, without

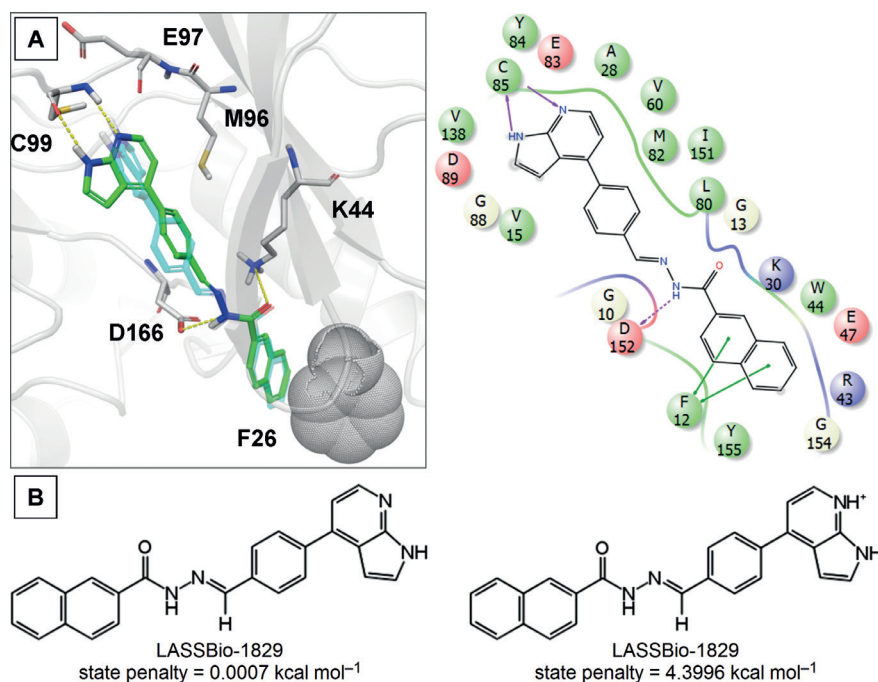
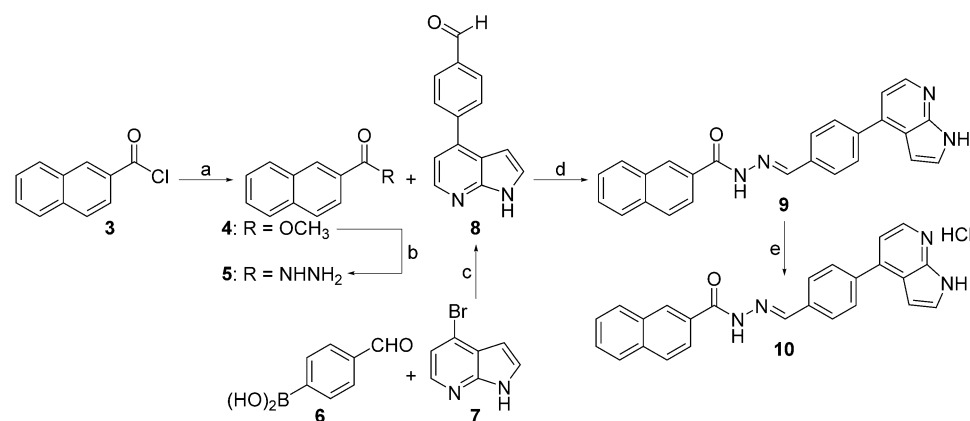


Figure 5. A) Docking results of the neutral (green) and protonated (cyan with transparency) forms of the compound LASSBio-1829 (left) and 2D ligand interaction diagram of its neutral form (right); note: residue position number labels on the 2D ligand interaction diagram are shifted by $n-14$ relative to residue numbering at left and in the text. B) Neutral and protonated structures of the NAH derivative LASSBio-1829 and their state penalties predicted by Epik.



Scheme 1. Reagents and conditions: a) MeOH, room temperature, 2 h, 86%; b) NH_2NH_2 , H_2O , 80% EtOH, reflux, 4 h, 82%; c) $\text{PdCl}_2(\text{PPh}_3)_2$, Na_2CO_3 , CH_3CN , H_2O , MW irradiation, 5 min, 65%; d) EtOH, 24 h, 75–80%; e) CH_3Cl , $\text{HCl}_{(\text{g})}$, 15–30 min, 15–50%.

the usual acid catalyst, to generate LASSBio-1829 (**9**) in good yield.^[37] The synthesis of the hydrochloride **10** was performed by bubbling hydrochloric acid gas in a chloroform solution containing LASSBio-1829 (**9**) (Scheme 1).

The double bond of NAH can be in the *E* or *Z* configuration.^[42] As already well established,^[43] the absence of duplication of the signals relating to amide and imine hydrogens of LASSBio-1829 (**9**) in the ^1H NMR spectrum is a strong indication that only the diastereomer presenting the relative configuration *E* was formed. The imine hydrogen atom in ^1H NMR spectra may appear to be doubled, but this profile results from two

different hydrogens being displayed within the same region. One is the imine hydrogen of NAH, and the other is the α -carbonyl hydrogen on the naphthyl core. This proposition was confirmed by analysis of the HSQC spectrum of LASSBio-1829 (see Supporting Information page S18). The hydrogen at 8.6 ppm is attached to the carbon in 147.68 ppm, corresponding to the imine carbon of NAH. The other hydrogen in 8.57 ppm is attached to a carbon at 143.16 ppm, referring to the carbon on the naphthyl nucleus.

Pharmacology

LASSBio-1829 (**9**) was evaluated for inhibition of IKK2 through in vitro tests by measuring the phosphorylation of phospho-I κ B- α -Ulight substrate using a human recombinant enzyme expressed in Sf21 cells.^[44] Unfortunately, this compound did not exhibit inhibitory activity. This might be due to the sensitivity of in vitro experiments to the aqueous solubility of the compounds tested.^[45] This hypothesis prompted us to propose that a lack of activity of this compound could be due to low water solubility. To improve the aqueous solubility of the compound, we proposed the synthesis of LASSBio-1829 hydrochloride (**10**). As expected, the hydrochloride **10** was 100-fold more soluble in water than the free base **9** (Table 1). In the same in vitro test, LASSBio-1829 hydrochloride (**10**) is active ($\text{IC}_{50} = 3.8 \mu\text{M}$) and more potent than the initial prototype, LASSBio-1524 ($\text{IC}_{50} = 20 \mu\text{M}$) (Table 1).

Subcutaneous air pouch (SAP) model

LASSBio-1829 (**9**) and hydrochloride LASSBio-1829 (**10**) were tested in in vivo models to confirm their possible anti-inflammatory action by inhibiting the NF- κ B-IKK2 pathway. The first model selected was the subcutaneous air pouch (SAP) in mice^[47] because this model has been described to activate NF-

| Compound | Aq. Sol. [mg mL ⁻¹] ^[a] | IC ₅₀ [μM] ^[b] |
|--------------------------------|--|--------------------------------------|
| LASSBio-1524 (1 a) | 1.20 × 10 ⁻³ | 20 |
| LASSBio-1829 (9) | 5.90 × 10 ⁻⁴ | ND |
| LASSBio-1829-HCl (10) | 5.54 × 10 ⁻² | 3.8 |
| Staurosporine ^[c] | ND | 0.52 |

[a] Solubility was determined by UV/Vis spectroscopy as described by Schneider et al.^[46] [b] Assay performed at Cerep (France). [c] Reference compound for IKK assay. ND: not determined.

κB in murine cells due to the inflammatory process induced by carrageenan.^[48]

Fortunately, both of the compounds showed good anti-inflammatory profiles in this model because they were both able to decrease, with differential potency, cell migration to the air pouch. At all of the doses tested, LASSBio-1829 (**9**) provided a decrease in cell migration, presenting a dose-response effect (Figure 6); however, only at the highest dose of LASSBio-1829,

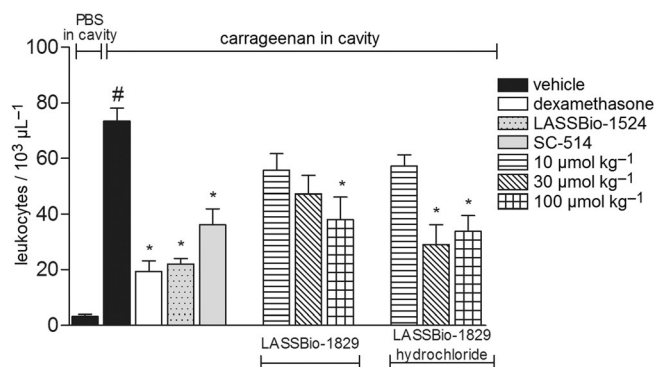


Figure 6. Effect of LASSBio-1829 (**9**) and LASSBio-1829 hydrochloride (**10**) on leukocyte migration induced by carrageenan in the subcutaneous air pouch (SAP). Animals were pretreated orally 60 min before carrageenan injection in the SAP with test compounds (at 10, 30, and 100 μmol kg⁻¹), dexamethasone (1.5 μmol kg⁻¹ i.p.), LASSBio-1524 (30 μmol kg⁻¹), SC-514 (30 μmol kg⁻¹ p.o.), or vehicle. Results are expressed as the mean ± SD of the number of total leukocytes. Statistical significance ($p < 0.05$) was calculated by analysis of variance (ANOVA) followed by Bonferroni post-test: # relative to the vehicle group that received phosphate-buffered saline (PBS) in SAP; * relative to the vehicle group that received carrageenan in SAP.

100 μmol kg⁻¹, was a significant decrease in cell migration to the pouch observed, by ~48%. As expected, LASSBio-1829 hydrochloride (**10**) was approximately twofold more potent than the respective free base **9**. At 30 and 100 μmol kg⁻¹ LASSBio-1829 hydrochloride (**10**) showed a significant decrease in cell migration, at 29 and 35%, respectively (Figure 6). The fact that the compounds were orally delivered in this model supports the hydrochloride synthesis strategy not only to enhance aqueous solubility but also to increase the intestinal absorption and bioavailability of the compound, resulting in a better cellular inhibition profile. The inhibitory behavior of LASSBio-1829 hydrochloride is consistent with that expected for IKK2

inhibitors, because two IKK2 inhibitors, LASSBio-1524 (**1 a**)^[25] and SC-514^[49] both at doses of 30 μmol kg⁻¹, showed similar potency to that of LASSBio-1829 hydrochloride (Figure 6), reducing cell migration by 23 and 46%, respectively.

TNF-α measurement

LASSBio-1829 hydrochloride (**10**) also showed an interesting anti-TNF-α activity in the air pouch exudate at a dose of 30 μmol kg⁻¹, inhibiting TNF-α migration by 46% (Figure 7). A decrease in TNF-α can be due to the IKK2 inhibitory action, whereas TNF-α expression is controlled by the NF-κB pathway, which involves activation of IKK2.^[50]

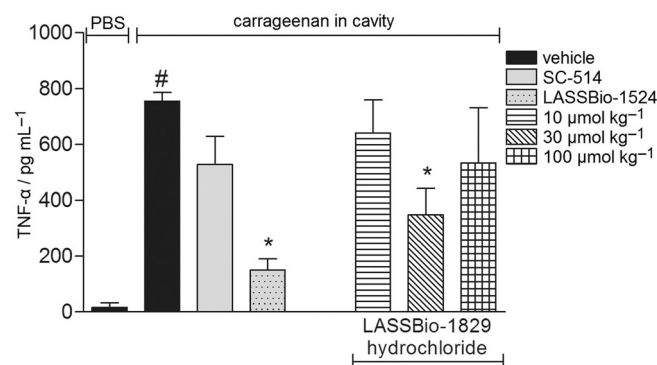


Figure 7. Effect of LASSBio-1829 hydrochloride (**10**) on the levels of TNF-α from exudate from the SAP. Animals were pretreated orally 60 min before carrageenan injection in the SAP, with compound **10** (10, 30, or 100 μmol kg⁻¹), LASSBio-1524 (30 μmol kg⁻¹), SC-514 (30 μmol kg⁻¹), or vehicle. Results are expressed as the mean ± SD of TNF-α concentration. Statistical significance ($p < 0.05$) was calculated by analysis of variance (ANOVA) followed by Bonferroni post-test: # relative to the vehicle group that received PBS in SAP; * relative to the vehicle group that received carrageenan in SAP.

Nitrate production

To access the inflammatory mediators involved with the NF-κB pathway that are produced during the inflammatory process and a possible effect of LASSBio-1829, the amount of nitric oxide (NO) that accumulated in the SAP exudate as nitrate was quantified. Figure 8 shows that the animals pretreated orally with vehicle and injected with phosphate-buffered saline (PBS) in SAP had significantly lower nitrate production. In the animals that received carrageenan injection in the SAP, pretreatment with the lowest dose of LASSBio-1829 hydrochloride was able to significantly decrease the production of NO relative to vehicle administration; however, higher concentrations of LASSBio-1829 hydrochloride were not able to decrease the production of NO.

Production of reactive oxygen species

The production of reactive oxygen species (ROS) is closely related to NF-κB activation.^[51,52] Therefore, the production of ROS was quantified in the animal air pouch treated with LASSBio-1829 hydrochloride. The compound had an excellent

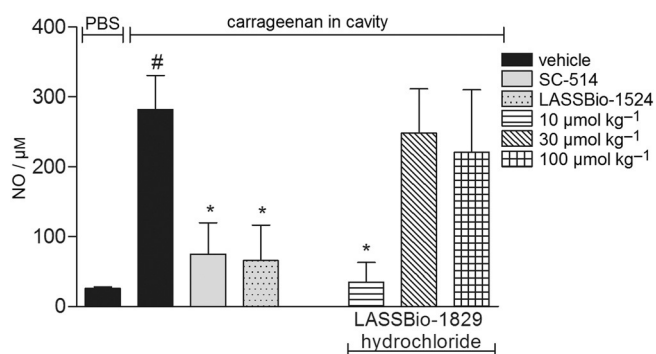


Figure 8. Effect of LASSBio-1829 hydrochloride (**10**) in nitric oxide (NO) production induced by carrageenan in the SAP. Animals were pretreated orally 60 min before carrageenan injection in the SAP with compound **10** (10, 30, or 100 $\mu\text{mol kg}^{-1}$), LASSBio-1524 (30 $\mu\text{mol kg}^{-1}$), SC-514 (30 $\mu\text{mol kg}^{-1}$), or vehicle. Results are expressed as the mean \pm SD of NO concentration. Statistical significance ($p < 0.05$) was calculated by ANOVA followed by Bonferroni post-test: # relative to the vehicle group that received PBS in SAP; * relative to the vehicle group that received carrageenan in SAP.

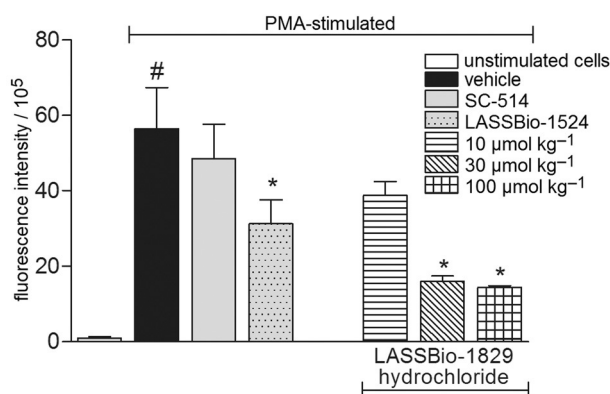


Figure 9. Effect of LASSBio-1829 hydrochloride (**10**), LASSBio-1524 (30 $\mu\text{mol kg}^{-1}$), and SC-514 (30 $\mu\text{mol kg}^{-1}$) on reactive oxygen species (ROS) production from leukocytes collected from the SAP 24 h after carrageenan injection and stimulated with phorbol myristate acetate (PMA). Reading was performed on a flow cytometer counting 10 000 events, and values shown are the geometric mean of fluorescence intensity expression of 2',7'-dichlorofluorescein (DCF) in the FL-1 channel. Statistical significance ($p < 0.05$) was calculated by ANOVA followed by Bonferroni post-test: # relative to the PMA-unstimulated vehicle group; * relative to the PMA-activated vehicle group.

dose–response profile, significantly decreasing ROS production at concentrations of 10 and 30 μM (Figure 9). LASSBio-1829 demonstrated a better pharmacological profile than LASSBio-1524 and SC-514 at 30 $\mu\text{mol kg}^{-1}$, consistent with its higher in vitro potency in relation to the other two IKK2 inhibitors.

Formalin test

LASSBio-1829 hydrochloride was submitted to the formalin test. The dose selected was 30 $\mu\text{mol kg}^{-1}$ because this dose appeared to be the most promising in the other tests. During the first phase of the formalin test, no significant action was observed. This lack of activity was expected because the inhibi-

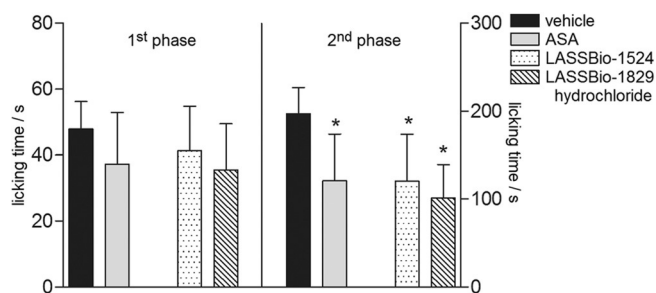


Figure 10. Effect of LASSBio-1829 hydrochloride (**10**) during the first and second phases of the formalin-induced licking response model. Animals were pretreated orally with compound **10** (30 $\mu\text{mol kg}^{-1}$), LASSBio-1524 (30 $\mu\text{mol kg}^{-1}$), acetylsalicylic acid (ASA, 1000 $\mu\text{mol kg}^{-1}$), or vehicle. Statistical significance ($p < 0.05$) was calculated by ANOVA followed by Bonferroni post-test: * relative to the vehicle group.

tion of the IKK2-NF- κ B pathway is not related to analgesia; however, during the second stage, where there is significant inflammatory involvement, the hydrochloride was able to minimize the licking number, once again confirming its good anti-inflammatory profile (Figure 10). LASSBio-1524 was also administered at the same dose (30 $\mu\text{mol kg}^{-1}$) as LASSBio-1829 and demonstrated pharmacological activity only during the second stage of the assay. This finding supports the hypothesis that IKK2 inhibitors are active only during the inflammatory phase in the formalin test. Acetylsalicylic acid (ASA), the positive control used in this test, reinforces this postulate. ASA has been reported to inhibit IKK2^[53] and, similar to LASSBio-1524 and LASSBio-1829, showed activity only during the inflammatory phase of the test.

Conclusions

In this work, we generated a three-dimensional model of IKK2 and exploited the profile of the ATP binding site through ATP and inhibitor docking studies. The molecular model built for IKK2 together with the docking methodology employed provided important and consistent information with respect to the structural and chemical inhibitor characteristics that may confer potency to IKK2 inhibitors. The docking results not only provided an explanation of the activity of compound LASSBio-1524 (**1a**) but also furnished important guidelines for the development of a new NAH inhibitor of IKK2. The docking results for LASSBio-1829 (**9**) predicted the presence of an important interaction with the hinge, the conserved residues Lys44 and Asp166, and stacking interactions with Phe26 from the G-loop. Furthermore, the analyses of the protonation states and the docking results indicate that LASSBio-1829 interacts with the enzyme in its neutral form. An important finding is that the aqueous solubility of LASSBio-1829 plays an important role in the determination of its potency. In fact, the inhibition of IKK2 through in vitro tests showed that only the hydrochloride of LASSBio-1829 (**10**) was active with an IC_{50} of 3.8 μM , showing more potent inhibition than the NAH prototype, LASSBio-1524. Additionally, during in vivo tests for inflammation with partici-

pation of the NF- κ B-IKK2 pathway, both compounds, LASSBio-1829 and LASSBio-1829 hydrochloride, were active; however, LASSBio-1829 hydrochloride is the most promising compound, showing superior potency. This result is likely due to their superior physicochemical profile, which can be seen in improved absorption, bioavailability and therapeutic action.

Experimental Section

Computational methods

Structural modeling of IKK2: Comparative modeling is a methodology that aims to generate 3D models of a protein sequence of interest (target) based on the primary sequences and using structures of similar proteins as templates.^[54,55] The molecular model of IKK2 was constructed with Modeller ver. 8^[56] through the multiple templates approach. The amino acid sequence of the protein target (IKK2) from *Homo sapiens* was extracted from the bank of sequences UniProt^[57] and stored with the code O14920. Because no high-quality structure is available that covers the entire sequence to be used as a template, only the catalytic domain of IKK2 was built (residues 15–300). Furthermore, the main focus of this work is the development of inhibitors that interact with the ATP binding site, which is located in the catalytic domain.

The search for sequences of homologous protein kinases to be used as templates was carried out with BLASTP^[58] using the BLOSUM62 matrix. For each isoform, a set of structures to be used in building the model was selected according to the following criteria: 1) high percentage of sequence identity (> 30%), 2) experimental structure with the ATP binding site well determined, 3) structural resolution less than or equal to 2.5 Å, and 4) absence of mutations. According to these criteria, three structures were selected as templates (PDB codes: 3BQR,^[59] 2A2A,^[60] and 1YHW^[61]) for building the IKK2 model (see details in Table S1, Supporting Information).

The three top-ranking models according to the DOPE energy provided by the Modeller program were selected for the step of loop optimization. Finally, the structural quality of the best energy model was analyzed using the MolProbity,^[62] QMEAN,^[63] and ProSA^[64,65] tools. MolProbity is largely employed to predict outlier residues on protein structures. ProSA uses force-field-based potentials to evaluate the accuracy of the protein structure according to statistical analyses of known structures of proteins. QMEAN is a validation tool that evaluates the quality of the protein structure according to geometrical factors.

The presence of conserved water and metal ions in the ATP binding site was analyzed through superimposition of diverse kinase-ATP/ADP/ANP complexes. Despite the high difference in the position of the metal ions between the complexes analyzed, kinetics studies demonstrated that a first cation is essential for phosphorylation of the ATP in most protein kinases.^[66] Nonetheless, this cation access is believed to provide the cofactor binding site complexed with ATP, justifying its absence in most inhibitor-kinase complexes.

The importance of water and metal ions in the ATP binding site was analyzed through docking studies of ATP in the presence and absence of water and ions. The water molecule (W397) and Mg²⁺ ion were extracted from the structure of the death-associated protein kinase 1 complexed with ANP (PDB code 3F5U^[67]).

Molecular docking simulations: Protein-ligand molecular docking is a widely used strategy that aims to predict the binding modes and affinities of one or more small molecules (ligands) in the binding site of a particular receptor (protein).^[68] The molecular docking experiments with the ATP cofactor were performed in the IKK2 binding site to validate the model built. The top ranked positions of the docking experiments were compared with the experimental conformation of ATP complexed with CDK2 (PDB code 1HCK^[30]). The docking experiments successfully determined the experimental binding mode of ATP only in the presence of a water molecule and the metal ion. This finding might indicate that the presence of at least one metal ion and a water molecule is important for ATP interaction in the IKK2 ATP binding site.

The docking studies of 18 inhibitors of IKK2 extracted from the BindingDB database^[69] were performed to achieve a better understanding of the properties that may confer their distinct potency and selectivity. The previously synthesized LASSBio-1524 (**1a**) and compound **1b**^[25] were docked into the IKK2 model to investigate the binding mode differences that could justify their distinct activity. The structures of the 18 inhibitors selected from the literature were obtained from the BindingDB^[69] and PubChem^[70] databases (Table S2), whereas the ATP and LASSBio compounds were manually designed in the Maestro Suite 2011 (version 9.2, Schrödinger LLC, New York, NY (USA), 2011). Only the *E* diastereomers of the LASSBio compounds were considered for the docking studies. All of the structures were prepared with LigPrep (version 2.5, Schrödinger LLC, 2011), and the protonation states were determined with Epik at pH 7.4 ± 4.0.^[71,72] The docking studies were performed with the Glide software (version 5.7, Schrödinger LLC, 2011) using the Extra Precision Docking mode.^[73]

Chemistry

General information: See the Supporting Information for details regarding reagents and equipment.

4-(1*H*-Pyrrolo[2,3-*b*]pyridin-4-yl)benzaldehyde (8**):** In a glass cylinder suitable for microwave reactions 4-bromo-1*H*-pyrrolo[2,3-*b*]pyridine (**7**, 0.2 g, 1.16 mmol, 1 equiv), 4-formylbenzeneboronic acid (**6**, 0.19 g, 1.27 mmol, 1.1 equiv), sodium carbonate (0.36 g, 3.74 mmol, 3 equiv) and catalyst (PdCl₂(PPh₃)₂) (0.04 g, 5.78 μmol, 0.05 equiv) were added. The reagents were then dissolved in 6 mL of a 1:1 solution of CH₃CN and H₂O, and the cylinder was inserted into the a microwave reactor, where it was heated for 5 min at 150 °C. After this time, TLC analysis revealed that the major product was the desired aldehyde **8**. The contents of the flask were transferred to a round-bottom flask, and the solvent was evaporated under reduced pressure. The solid obtained was purified by column chromatography with the eluent *n*-hexane/EtOAc (5–50%) to provide the desired aldehyde **8** in 65% yield. ¹H NMR (200 MHz, [D₆]DMSO): δ = 11.90 (1H, s), 10.10 (1H, s), 8.35 (1H, d, *J* = 6 Hz), 8.11 (2H, d, *J* = 8 Hz), 8.02 (2H, d, *J* = 8 Hz), 7.61 (1H, m), 7.29 (1H, d, *J* = 6 Hz), 6.66 ppm (1H, d, *J* = 4 Hz); ¹³C NMR (50 MHz, [D₆]DMSO): δ = 194.7, 149.4, 145.1, 143.7, 140.5, 136.6, 131.3, 130.0, 128.4, 118.5, 115.6, 100.2 ppm; IR (KBr): $\tilde{\nu}$ = 3135 and 3079 (N–H), 2772 and 2877 (C–H), 1705 cm⁻¹ (C=O).

(*E*)-*N*-(4-(1*H*-Pyrrolo[2,3-*b*]pyridin-4-yl)benzylidene)-2-naphthohydrazide (9**, LASSBio-1829):** To a solution of 2-naphthohydrazide (**5**, 0.17 g, 92.9 μmol, 1 equiv) in absolute EtOH (15 mL) aldehyde **8** was added (0.19 g, 86.9 μmol, 1 equiv). The mixture was stirred at room temperature for 24 h. Afterward, the solvent was partially concentrated at reduced pressure, and the resulting mixture was poured into ice and cold water. The precipitate formed was filtered

out and dried under vacuum, producing the desired *N*-acylhydrazone in 80% yield. ¹H NMR (400 MHz, [D₆]DMSO): δ = 12.13 (1 H, s), 11.80 (1 H, s), 8.58 (1 H, s), 8.56 (1 H, s), 8.29 (1 H, d, *J* = 4 Hz), 8.01–8.05 (2 H, m), 7.99 (2 H, d, *J* = 8 Hz), 7.94 (2 H, d, *J* = 8 Hz), 7.88 (2 H, d, *J* = 8 Hz), 7.61–7.66 (2 H, m), 7.56 (1 H, s), 7.24 (1 H, d, *J* = 4 Hz), 6.67 ppm (1 H, s); ¹³C NMR (50 MHz, [D₆]DMSO + CDCl₃): δ = 163.5, 149.0, 147.5, 142.8, 140.1, 139.7, 134.4, 134.3, 132.1, 130.6, 128.9, 128.6, 128.1, 127.9, 127.7, 127.7, 126.9, 126.7, 124.3, 117.3, 114.1, 99.1 ppm; IR (KBr): $\tilde{\nu}$ = 1648 (C=O), 3440, 3199, 3138 cm⁻¹ (N–H); HPLC: 96.56% purity; MS: *m/z* = 391.1 [*M* + H]⁺.

(*E*)-*N*-(4-(1*H*-Pyrrolo[2,3-*b*]pyridin-4-yl)benzylidene)-2-naphthohydrazide hydrochloride (10, LASSBio-1829 hydrochloride): In a flask containing 0.70 g LASSBio-1829 (**9**), CHCl₃ was added (150 mL), and the solution was transferred to magnetic stirring. Hydrochloric acid gas was bubbled into the flask for 30 min. During the reaction the hydrochloride precipitated as a yellow solid. After the solvent was evaporated under reduced pressure, Et₂O was added to the flask and vacuum filtered, obtaining LASSBio-1829 hydrochloride (**10**) in 50% yield. ¹H NMR 200 MHz, [D₆]DMSO): δ = 12.18 (1 H, s), 8.61 (1 H, s), 8.58 (1 H, s), 8.41 (1 H, d, *J* = 6 Hz), 7.95–8.23 (8 H, m), 7.63–7.67 (3 H, m), 7.35–7.42 (1 H, m), 6.78 ppm (1 H, m); HPLC: 96.44% purity.

Pharmacology

Animals: The experimental groups were composed of 5–8 female Swiss Webster mice of 20–25 g donated by the Animal Production Centre of the Institute Vital Brazil. The experimental protocols followed the rules advocated by Law 11.794, of October 8, 2008 by the National Council of Animal Experimentation Control (CONCEA) and were approved by the Ethics Committee of Animal Use (CEUA), Science Center Health/UFRJ number DFBCICB015–04/16.

Preparation and administration of compounds: LASSBio-1829 and LASSBio-1829 hydrochloride were prepared in a stock solution of 100 μmol in 1 mL DMSO and stored at –20 °C. The compounds were administered orally at doses of 10, 30, or 100 μmol kg⁻¹ in a final volume of 100 μL vehicle (Polysorbate 80). LASSBio-1524 and the selective and reversible IKK2 inhibitor SC-514^[74] were administered orally at a single dose of 30 μmol kg⁻¹. The standard anti-inflammatory medications used were dexamethasone (1.5 μmol kg⁻¹) and acetylsalicylic acid (ASA, 1000 μmol kg⁻¹, p.o.).

Subcutaneous air pouch (SAP) model: The formation of an air pouch in the dorsum of mice was carried out upon injection of 10 mL sterile air a 1% carrageenan solution, a phlogistic agent, to induce cell migration.^[47] After 3 days, over 7 mL of sterile air were injected. On day 6, the animals were treated with compounds, and 60 min later, a sterile 1% carrageenan injection was made in the formed cavity. A negative control group was treated with vehicle 60 min before receiving the injection of the sterile carrageenan solution at SAP, and the positive control group received dexamethasone and SC-514. 24 h post-carrageenan injection, animals were euthanized, and the cavity was washed with 1 mL phosphate-buffered saline (PBS). The number of cells from the collected exudate was then determined with an automatic cell counter (Poch-100iV Diff, Sysmex). The exudate was centrifuged at 1000 rpm for 10 min at 4 °C. The supernatant was stored at –20 °C until subsequent measurements.

TNF-α measurement: Quantification of TNF-α was carried out for the SAP exudate. The ELISA kit BD ELISA OptEIAM was used, and the TNF-α concentration was determined according to the manufacturer's recommendations (B&D Biosciences). The absorbance was measured at λ 450 nm using a microplate reader, and the cyto-

kine concentrations were calculated using a standard curve and are expressed as pg mL⁻¹.

Production of nitric oxide: NO produced in the SAP supernatant was quantified according to the technique of the conversion of nitrate to nitrite.^[46] The SAP samples were deproteinized and then admixed to a sample of sodium phosphate (0.5 M, pH 7.2), ammonium formate (2.4 M, pH 7.2), and *E. coli*. After incubation for 2 h at 37 °C, centrifugation was performed at 10000 rpm for 10 min. Equal portions of the supernatant and Griess reagent were incubated for 10 min,^[75] and the absorbance was measured spectrophotometrically at λ 540 nm. The nitrate concentration values are expressed in nanomolar and were calculated from a standard curve of sodium nitrate.

Determination of reactive oxygen species (ROS) production: Leukocytes collected in the SAP were placed in tubes (10⁶ cells) in a volume of 1 mL. Incubation was performed at 37 °C and 5% CO₂ for 1 h. Test compounds were then added at concentrations of 1, 10, and 30 μM and incubated for 30 min at 37 °C and 5% CO₂. The cells were treated with 10 nM phorbol myristate acetate (PMA) and incubated for 45 min at 37 °C and 5% CO₂. The cells were then added to 2',7'-dichlorodihydrofluorescein diacetate (DCF-DA, 2 mM), followed by another incubation for 30 min at 37 °C. DCF-DA quickly permeates the cell membrane, and once in the intracellular space, is hydrolyzed by plasma esterase, to be converted into 2',7'-dichlorofluorescein (DCFH), which is a non-fluorescent compound that is impermeable to the cell membrane. In the presence of ROS, DCFH is oxidized within the cell and produces a fluorescent compound, 2',7'-dichlorofluorescein (DCF), which remains in the extracellular space.^[76] The emitted fluorescence is captured in the FL-1 channel of a flow cytometer and is expressed in arbitrary units (au).

Formalin test: Animals received an injection of formalin (2.5% v/v) into their left hind paws. The time that the animals spent licking their paws after injection was recorded. The nociceptive response develops during two phases: 0–5 min after the formalin injection (first phase, neurogenic pain response) and 15–30 min after the formalin injection (second phase, inflammatory pain response).

Statistical analysis: All of the experiments were composed of 6–8 randomly selected animals per group. The results are presented as the mean ± standard deviation (SD). Statistical significance was calculated by analysis of variance (ANOVA) followed by Bonferroni post-test, using GraphPad Prism ver. 5.0 software; significance was considered at *p* < 0.05.

Acknowledgements

The authors thank Instituto Nacional de Ciência e Tecnologia de Fármacos e Medicamentos (INCT-INOVAR) (grants 573.564/2008-6 and 170.020/2008), Fundação Carlos Chagas Filho de Amparo à Pesquisa do Estado do Rio de Janeiro (FAPERJ), and Conselho Nacional de Desenvolvimento Científico e Tecnológico (CNPq) for financial support. The authors also thank the Institute Vital Brazil for animal donation, Coordenadoria de Aperfeiçoamento de Pessoal de Nível Superior (CAPES) for fellowships to N.S.C. and R.H.C.N.F., and Alan Minho (Institute of Biomedical Sciences, UFRJ) for technical support.

Keywords: anti-inflammatory agents · IKK2 · molecular docking · *N*-acylhydrazones · structure-based drug design

- [1] D. M. Rothwarf, E. Zandi, G. Natoli, M. Karin, *Nature* **1998**, *395*, 297–300.
- [2] S. Yamaoka, G. Courtois, C. Bessia, S. T. Whiteside, R. Weil, F. Agou, H. E. Kirk, R. J. Kay, A. Israël, *Cell* **1998**, *93*, 1231–1240.
- [3] E. Zandi, D. M. Rothwarf, M. Delhase, M. Hayakawa, M. Karin, *Cell* **1997**, *91*, 243–252.
- [4] R. M. Townsend, J. Postelnek, V. Susulic, K. W. McIntyre, D. J. Shuster, Y. Qiu, F. C. Zusi, J. R. Burke, *Transplantation* **2004**, *77*, 1090–1094.
- [5] J. A. Schmid, A. Birbach, *Cytokine Growth Factor Rev.* **2008**, *19*, 157–165.
- [6] A. Israel, *Cold Spring Harbor Perspect. Biol.* **2010**, *2*, a000158–a000158.
- [7] J.-L. Luo, H. Kamata, M. Karin, *J. Clin. Invest.* **2005**, *115*, 2625–2632.
- [8] C. H. Lee, Y.-T. Jeon, S.-H. Kim, Y.-S. Song, *Biofactors* **2007**, *29*, 19–35.
- [9] M. C.-T. Huo, D.-F. Lee, W. Xia, L. S. Golfman, F. Ou-Yang, J.-Y. Yang, Y. Zou, S. Bao, N. Hanada, H. Saso, R. Kobayashi, M. C. Hung, *Cell* **2004**, *117*, 225–237.
- [10] H. J. Kim, N. Hawke, A. S. Baldwin, *Cell Death Differ.* **2006**, *13*, 738–747.
- [11] J. Strnad, J. R. Burke, *Trends Pharmacol. Sci.* **2007**, *28*, 142–148.
- [12] S. Uota, M. Zahidunnabi Dewan, Y. Saitoh, S. Muto, A. Itai, A. Utsunomiya, T. Watanabe, N. Yamamoto, S. Yamaoka, *Cancer Sci.* **2012**, *103*, 100–106.
- [13] Y. Yamamoto, R. B. Gaynor, *J. Clin. Invest.* **2001**, *107*, 135–142.
- [14] S. Ghosh, M. Karin, *Cell* **2002**, *109*, 581–96.
- [15] Q. Li, I. M. Verma, *Nat. Rev. Immunol.* **2002**, *2*, 725–734.
- [16] S. Vallabhapurapu, M. Karin, *Annu. Rev. Immunol.* **2009**, *27*, 693–733.
- [17] G. Courtois, T. D. Gilmore, *Oncogene* **2006**, *25*, 6831–6843.
- [18] A. Oeckinghaus, S. Ghosh, *Cold Spring Harbor Perspect. Biol.* **2009**, *1*, a000034.
- [19] M. Karin, M. Delhase, *Semin. Immunol.* **2000**, *12*, 85–98.
- [20] G. W. Peet, J. Li, *J. Biol. Chem.* **1999**, *274*, 32655–32661.
- [21] Y. Hu, V. Baud, T. Oga, K. I. Kim, K. Yoshida, M. Karin, *Nature* **2001**, *410*, 710–714.
- [22] G. Xu, Y.-C. Lo, Q. Li, G. Napolitano, X. Wu, X. Jiang, M. Dreano, M. Karin, H. Wu, *Nature* **2011**, *472*, 325–330.
- [23] S. Polley, D.-B. Huang, A. V. Hauenstein, A. J. Fusco, X. Zhong, D. Vu, B. Schröfelbauer, Y. Kim, A. Hoffmann, I. M. Verma, G. Ghosh, T. Huxford, *PLoS Biol.* **2013**, *11*, e1001581.
- [24] S. Liu, Y. R. Misquitta, A. Olland, M. A. Johnson, K. S. Kelleher, R. Kriz, L. L. Lin, M. Stahl, L. Mosyak, *J. Biol. Chem.* **2013**, *288*, 22758–22767.
- [25] C. M. Avila, A. B. Lopes, A. S. Gonçalves, L. L. da Silva, N. C. Romeiro, A. L. P. Miranda, C. M. R. Sant’Anna, E. J. Barreiro, C. A. M. Fraga, *Eur. J. Med. Chem.* **2011**, *46*, 1245–1253.
- [26] G. Scapin, S. B. Patel, J. Lisnock, J. W. Becker, P. V. LoGrasso, *Chem. Biol.* **2003**, *10*, 705–712.
- [27] A. P. Kornev, N. M. Haste, S. S. Taylor, L. F. T. Eyck, *Proc. Natl. Acad. Sci. USA* **2006**, *103*, 17783–17788.
- [28] R. Roskoski, *Expert Opin. Drug Discovery* **2013**, *8*, 1165–1179.
- [29] K. C. Duong-Ly, J. R. Peterson, *Curr. Protoc. Pharmacol.* **2013**, *60*, 2.9.1–2.9.14.
- [30] U. Schulze-Gahmen, H. L. De Bondt, S.-H. Kim, *J. Med. Chem.* **1996**, *39*, 4540–4546.
- [31] C. Zhang, S.-H. Kim in *Computational and Structural Approaches to Drug Discovery: Ligand–Protein Interactions* (Eds.: R. Stroud, J. Finer-Moore), Royal Society of Chemistry, Cambridge, **2007**, pp. 349–365.
- [32] L. Garuti, M. Roberti, G. Bottegoni, *Curr. Med. Chem.* **2010**, *17*, 2804–2821.
- [33] L. K. Gavrin, E. Saiah, *MedChemComm* **2013**, *4*, 41–51.
- [34] D. Fancelli, D. Berta, S. Bindi, A. Cameron, P. Cappella, P. Carpinelli, C. Catana, B. Forte, P. Giordano, M. L. Giorgini, S. Mantegani, A. Marsiglio, M. Merone, J. Moll, V. Pitallà, F. Roletto, D. Severino, C. Soncini, P. Storicci, R. Tonani, M. Varasi, A. Vulpetti, P. Vianello, *J. Med. Chem.* **2005**, *48*, 3080–3084.
- [35] A. H. Bingham, R. J. Davenport, L. Gowers, R. L. Knight, C. Lowe, D. A. Owen, D. M. Parry, W. R. Pitty, *Bioorg. Med. Chem. Lett.* **2004**, *14*, 409–412.
- [36] C. D. Duarte, E. J. Barreiro, C. A. M. Fraga, *Mini-Rev. Med. Chem.* **2007**, *7*, 1108–1119.
- [37] P. C. Lima, L. M. Lima, K. C. da Silva, P. H. Léda, A. L. de Miranda, C. A. M. Fraga, E. J. Barreiro, *Eur. J. Med. Chem.* **2000**, *35*, 187–203.
- [38] A. Suzuki, *Pure Appl. Chem.* **1994**, *66*, 213–222.
- [39] H. Peng, T. Talreja, Z. Xin, J. H. Cuervo, G. Kumaravel, M. J. Humora, L. Xu, E. Rohde, L. Gan, M.-Y. Jung, M. N. Shackett, S. Chollate, A. W. Dunah, P. A. Snodgrass-belt, H. M. Arnold, A. G. Taveras, K. J. Rhodes, R. H. Scannevin, *ACS Med. Chem. Lett.* **2011**, *2*, 786–791.
- [40] H. Suzuki, I. Utsunomiya, K. Shudo, T. Fujimura, M. Tsuji, I. Kato, T. Aoki, A. Ino, T. Iwaki, *ACS Med. Chem. Lett.* **2013**, *4*, 1074–1078.
- [41] Y. Gong, W. He, *Org. Lett.* **2002**, *4*, 3803–3805.
- [42] G. Palla, G. Predieri, P. Domiano, C. Vignali, W. Turner, *Tetrahedron* **1986**, *42*, 3649–3654.
- [43] G. Palla, C. Pelizzi, G. Predieri, *Gazz. Chim. Ital.* **1982**, *112*, 339–341.
- [44] Q. K. Huynh, H. Boddupalli, S. A. Rouw, C. M. Koboldt, T. Hall, C. Sommers, S. D. Hauser, J. L. Pierce, R. G. Combs, B. A. Reitz, J. A. Diaz-Collier, R. A. Weinberg, B. L. Hood, B. F. Kilpatrick, C. S. Tripp, *J. Biol. Chem.* **2000**, *275*, 25883–25891.
- [45] J. B. Dressman, C. Reppas, *Eur. J. Pharm. Sci.* **2000**, *11*, S73–S80.
- [46] P. Schneider, S. S. Hosseiny, M. Szczotka, V. Jordan, K. Schlitter, *Phytochem. Lett.* **2009**, *2*, 85–87.
- [47] L. J. R. P. Raymundo, C. C. Guilhon, D. S. Alviano, M. E. Matheus, A. R. Antonioli, S. C. H. Cavalcanti, P. B. Alves, C. S. Alviano, P. D. Fernandes, *J. Ethnopharmacol.* **2011**, *134*, 725–732.
- [48] L. Ellis, C. C. Y. Soo, C. J. Morris, B. L. Kidd, P. G. Winyard, *Ann. Rheum. Dis.* **2000**, *59*, 303–307.
- [49] A. Baxter, S. Brough, A. Cooper, E. Floettmann, S. Foster, C. Harding, J. Kettle, T. McNally, C. Martin, M. Mobbs, M. Needham, P. Newham, S. Paine, S. St-Gallay, S. Salter, J. Unitt, Y. Xue, *Bioorg. Med. Chem. Lett.* **2004**, *14*, 2817–2822.
- [50] S. C. Gupta, C. Sundaram, S. Reuter, B. B. Aggarwal, *BBA-Gene Regul. Mech.* **2010**, *1799*, 775–787.
- [51] C. Bubici, S. Papa, K. Dean, G. Franzoso, *Oncogene* **2006**, *25*, 6731–6748.
- [52] M. J. Morgan, Z. Liu, *Cell Res.* **2011**, *21*, 103–115.
- [53] M.-J. Yin, Y. Yamamoto, R. B. Gaynor, *Nature* **1998**, *396*, 77–80.
- [54] M. A. Martí-Renom, A. C. Stuart, A. Fiser, R. Sánchez, F. Melo, A. Sali, *Annu. Rev. Biophys. Biomol. Struct.* **2000**, *29*, 291–325.
- [55] M. S. Madhusudhan, M. A. Martí-Renom, N. Eswar, B. John, U. Pieper, R. Karchin, M. Shen, A. Sali, *Comparative Protein Structure Modeling* (Ed.: J. M. Walker), The Proteomics Protocols Handbook, Humana Press Inc., Totowa, NJ, **2005**, 831–860.
- [56] A. Sali, T. L. Blundell, *J. Mol. Biol.* **1993**, *234*, 779–815.
- [57] The UniProt Consortium, *Nucleic Acids Res.* **2015**, *43*, D204–D212.
- [58] S. F. Altschul, W. Gish, W. Miller, E. W. Myers, D. J. Lipman, *J. Mol. Biol.* **1990**, *215*, 403–410.
- [59] “Crystal Structure of Human Death Associated Protein Kinase 3 (DAPK3) in Complex with an Imidazo-Pyridazine Ligand”, P. Filippakopoulos, P. Rellos, O. Fedorov, F. Niesen, A. C. W. Pike, E. S. Pilka, F. von Delft, C. H. Arrowsmith, A. M. Edwards, J. Weigelt, S. Knapp, PDB ID 3BQR: <http://pdb.org/pdb/explore/explore.do?structureId=3bqr>, DOI: 10.2210/pdb3bqr/pdb.
- [60] “High-Resolution Analysis of the Autoinhibited Conformation of Human DRP-1 Kinase”, P. Kursula, M. Wilmanns, PDB ID 2A2A: <http://pdb.org/pdb/explore/explore.do?structureId=2a2a>, DOI: 10.2210/pdb2a2a/pdb.
- [61] M. Lei, M. A. Robinson, S. C. Harrison, *Structure* **2005**, *13*, 769–778.
- [62] V. B. Chen, W. B. Arendall III, J. J. Headd, D. A. Keedy, R. M. Immormino, G. J. Kapral, L. W. Murray, J. S. Richardson, D. C. Richardson, *Acta Crystallogr. Sect. D* **2010**, *66*, 12–21.
- [63] P. Benkert, T. Schwede, S. C. E. Tosatto, *BMC Struct. Biol.* **2009**, *9*, 35.
- [64] M. Wiederstein, M. J. Sippl, *Nucleic Acids Res.* **2007**, *35*, W407–410.
- [65] M. J. Sippl, *Proteins* **1993**, *17*, 355–362.
- [66] J. A. Adams, *Chem. Rev.* **2001**, *101*, 2271–2290.
- [67] L. K. McNamara, D. M. Watterson, J. S. Brunzelle, *Acta Crystallogr. Sect. D* **2009**, *65*, 241–248.
- [68] I. A. Guedes, C. S. de Magalhães, L. E. Dardenne, *Biophys. Rev.* **2014**, *6*, 75–87.
- [69] T. Liu, Y. Lin, X. Wen, R. N. Jorissen, M. K. Gilson, *Nucleic Acids Res.* **2007**, *35*, D198–D201.
- [70] E. E. Bolton, Y. Wang, P. A. Thiessen, S. H. Bryant, *Annu. Rep. Comput. Chem.* **2008**, *4*, 217–241.
- [71] J. R. Greenwood, D. Calkins, A. P. Sullivan, J. C. Shelley, *J. Comput.-Aided Mol. Des.* **2010**, *24*, 591–604.
- [72] J. C. Shelley, A. Cholleti, L. L. Frye, J. R. Greenwood, M. R. Timlin, M. Uchimaya, *J. Comput.-Aided Mol. Des.* **2007**, *21*, 681–691.

- [73] R. A. Friesner, R. B. Murphy, M. P. Repasky, L. L. Frye, J. R. Greenwood, T. A. Halgren, P. C. Sanschagrín, D. T. Mainz, *J. Med. Chem.* **2006**, *49*, 6177–6196.
- [74] N. Kishore, C. Sommers, S. Mathialagan, J. Guzova, M. Yao, S. Hauser, K. Huynh, S. Bonar, C. Mielke, L. Albee, R. Weier, M. Graneto, C. Hanau, T. Perry, C. S. Tripp, *J. Biol. Chem.* **2003**, *278*, 32861–32871.
- [75] L. C. Green, D. A. Wagner, J. Glogowski, P. L. Skipper, J. S. Wishnok, S. R. Tannenbaum, *Anal. Biochem.* **1982**, *126*, 131–138.
- [76] N. Srivastava, V. K. Gonugunta, M. R. Puli, A. S. Raghavendra, *Planta* **2009**, *229*, 757–765.

Received: June 18, 2015

Revised: August 5, 2015

Published online on August 25, 2015